



# Novel anoikis-related genes for the diagnosis of non-obstructive azoospermia

Xiaolian Xu<sup>1</sup>, Jinlong Xie<sup>2</sup>, Wenchang Cheng<sup>3</sup>

<sup>1</sup>Electrophysiology Laboratory, Affiliated Hospital of Shandong Second Medical University, Weifang, China; <sup>2</sup>The Reproductive Medicine Center of Weifang People's Hospital, Shandong Second Medical University, Weifang, China; <sup>3</sup>Department of Urology, Affiliated Hospital of Shandong Second Medical University, Weifang, China

**Contributions:** (I) Conception and design: W Cheng, X Xu; (II) Administrative support: W Cheng, X Xu; (III) Provision of study materials or patients: All authors; (IV) Collection and assembly of data: All authors; (V) Data analysis and interpretation: W Cheng, X Xu; (VI) Manuscript writing: All authors; (VII) Final approval of manuscript: All authors.

**Correspondence to:** Wenchang Cheng, MD. Department of Urology, Affiliated Hospital of Shandong Second Medical University, No. 2428 Yuhe Road, Weifang 261031, China. Email: wfcwc1986@163.com.

**Background:** Non-obstructive azoospermia (NOA) is a prevalent cause of male infertility, featured by the absence of sperm in the ejaculate due to impaired spermatogenesis. The involvement of anoikis in the pathogenesis of NOA remains inadequately understood. This research aims to identify anoikis-related genes as potential biomarkers for NOA diagnosis.

**Methods:** Based on the Gene Expression Omnibus (GEO) database and Limma R package, we identified differentially expressed genes of NOA and downloaded anoikis-related genes based on the GeneCards database. Subsequently, anoikis-related hub genes were screened by machine learning (ML), and validated using external validation sets. A nomogram constructed from these genes demonstrated high predictive accuracy, while boxplots and complex heatmaps illustrated the differential expression patterns observed in NOA samples. Additionally, immune infiltration analysis was performed using the CIBERSORT algorithm to evaluate the distribution of immune cells in both NOA and control groups. The validation of candidate genes was conducted through receiver operating characteristic (ROC) curve analysis, with the area under the curve (AUC) indicating predictive accuracy.

**Results:** Ultimately, we screened three hub genes: *GLO1*, *BAP1*, and *PLK1*. *GLO1* was found to be up-regulated, while both *BAP1* and *PLK1* were down-regulated. Immune cell infiltration analysis elicited significant differences in 16 immune cell types between NOA patients and normal controls, with Tregs and macrophages notably up-regulated in NOA. ROC analysis indicated that all the three hub genes exhibited excellent diagnostic efficacy. Specifically, ROC curve analysis confirmed the diagnostic potential of *GLO1*, *BAP1*, and *PLK1*, yielding AUC values of 0.981, 0.980, and 0.981 in internal datasets, and 0.750, 0.875, and 1.000 in external datasets.

**Conclusions:** By ML analysis, this research identified three anoikis-related genes that may be diagnostic biomarkers for NOA, offering views into the underlying molecular mechanisms and therapeutic targets.

**Keywords:** Anoikis-related genes; non-obstructive azoospermia (NOA); random forest (RF); support vector machine (SVM)

Submitted Dec 20, 2024. Accepted for publication Mar 24, 2025. Published online Apr 27, 2025.

doi: 10.21037/tau-2024-745

**View this article at:** <https://dx.doi.org/10.21037/tau-2024-745>

## Introduction

### Background

Male infertility represents a significant reproductive health issue, affecting approximately 15% of individuals of reproductive age (1). Among the conditions contributing to male infertility, non-obstructive azoospermia (NOA) is particularly noteworthy, marked by the dearth of sperm in the ejaculate due to impaired spermatogenesis, accounting for 10–15% of all cases of male infertility (2). This condition poses profound psychological and emotional challenges for the affected males and represents a considerable economic burden on healthcare systems and society, particularly in the context of the increasing prevalence of infertility issues. Current diagnostic and therapeutic approaches for NOA, including hormonal assessments, testicular biopsy, and microdissection testicular sperm extraction are often ineffective and fail to address the underlying molecular mechanisms of NOA (3,4). Furthermore, the lack of specificity and sensitivity of existing methods impedes accurate diagnosis and effective treatment. Currently, no effective pharmacological therapies have been established for NOA. Consequently, innovative strategies are urgently needed to deepen our understanding of the molecular landscape of NOA.

### Highlight box

#### Key findings

- Using machine learning (ML) techniques, specifically support vector machines and random forests, we identified three pivotal genes—*GLO1*, *BAP1*, and *PLK1*—that exhibit significant diagnostic potential and highlight the biological processes and associated pathways pertinent to the molecular mechanisms underlying non-obstructive azoospermia (NOA).

#### What is known and what is new?

- Identifying anoikis-related genes associated with NOA using ML presents a significant challenge; however, this innovative diagnostic tool warrants further investigation.
- The application of ML has successfully revealed three Novel anoikis-related genes, thereby offering new insights into the underlying mechanisms and diagnostic processes for NOA.

#### What is the implication, and what should change now?

- Through ML analysis, we identified three anoikis-related genes that may serve as diagnostic biomarkers for NOA. Future studies should incorporate wet lab experiments and larger cohorts to enhance the robustness of the findings and validate the identified biomarkers in clinical settings.

### Rationale and knowledge gap

Anoikis is an integrin-dependent mode of cell death that is crucial in diverse physiological and pathological processes, like embryonic development, organ development, tissue repair, inflammatory responses, cardiovascular diseases, and tumor metastasis (5). Anoikis was first discovered in 1994 by disrupting the interplay between normal epithelial cells and extracellular matrix (ECM) (6). According to current views, anoikis is primarily mediated by membrane adhesion signaling molecules, specifically integrin family proteins. As a result, anoikis can respond to physical and chemical stimuli and may cross-talk via integrins within the same downstream signaling pathways (5). Furthermore, anoikis is influenced by various molecular pathways, including STAT3 (7), TrkB (8), Wnt (9), and Hippo (10), as well as noncoding RNAs, epigenetic modifications, and ECM regulation processes. Previous research has established a link between apoptosis and male infertility (11), yet the specific role of anoikis—a specific form of cell apoptosis, in anchorage-dependent cells—remains underexplored in NOA. Anoikis may be critical in the pathogenesis of spermatogenic failure, which warrants further investigations (*Figure 1*).

### Objective

This study employs a comprehensive bioinformatics approach to identify anoikis-related genes that may be potential biomarkers for diagnosing NOA. This methodology integrates differential gene expression analysis, functional enrichment assessments, and machine learning (ML) techniques, which collectively enhance the robustness of the findings. Notably, three critical anoikis-related genes were pinpointed, which exhibited high diagnostic efficacy, as evidenced by their high area under the curve (AUC) in both internal and external validation datasets. These findings underline the potential of anoikis-related genes as novel diagnostic markers for NOA, laying the foundation for future research to elucidate their mechanistic roles in male infertility. We present this article in accordance with the STARD reporting checklist (available at <https://tau.amegroups.com/article/view/10.21037/tau-2024-745/rc>).

## Methods

### Data collection

Four datasets GSE45885, GSE45887, GSE145467, and

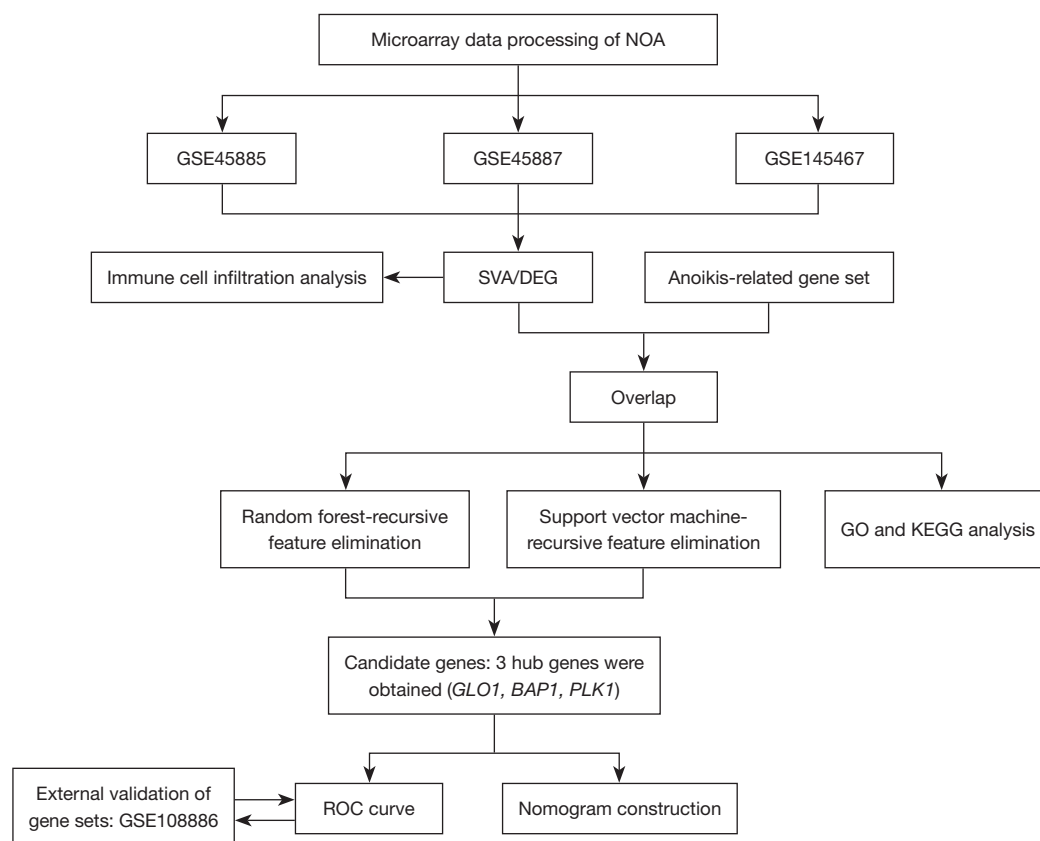


**Figure 1** Flowchart of this study. DEG, differentially expressed gene; GO, gene ontology; KEGG, Kyoto Encyclopedia of Genes and Genomes; NOA, non-obstructive azoospermia; ROC, receiver operating characteristic; SVA, Surrogate Variable Analysis.

GSE108886 on NOA were acquired from the public database GEO (<http://www.ncbi.nlm.nih.gov/geo/>) (12). These datasets comprised 61 NOA samples and 19 normal spermatogenesis samples, which were all sourced from testicular biopsy specimens. The microarray information of these datasets was obtained and organized using the GEOquery package (13). The expression matrices were corrected and normalized using R. The three datasets, GSE45885, GSE45887, and GSE145467, served as the training set, and GSE108886 served as the external validation set. The study was conducted in accordance with the Declaration of Helsinki and its subsequent amendments.

R 4.4.1 (<https://www.r-project.org/>) and the ComBat function (14) of the Surrogate Variable Analysis (SVA) package were leveraged to integrate the data from the three training datasets, and 53 NOA samples and 18 normal samples were obtained by removing the batch effect and merging the data (15). The limma package (16) was employed for differential gene analysis, with 16,105

differentially expressed genes (DEGs) screened using the thresholds of  $|\log\text{fold change (FC)}| > 1$  and  $\text{adj.P.Val} < 0.05$ . The screened DEGs were shown in volcano plots using the ggplot2 package.

Anoikis-related genes were downloaded from the GeneCards database (<https://www.genecards.org/>). A total of 919 anoikis-related genes were intersected with DEGs, and anoikis-related DEGs were shown in a Venn diagram using the VennDiagram package (Table 1).

#### ***Random forest-recursive feature elimination (RF-RFE)/support vector machine-recursive feature elimination (SVM-RFE)***

SVM-RFE analysis is a supervised ML technique that identifies the optimal gene by eliminating the feature vectors generated by SVM (17). RF-RFE analysis is a decision tree-based ML method that evaluates variables by scoring their importance (18). RF and SVM algorithms

**Table 1** Sample information of NOA dataset

Dataset	Database	Platform	Sample	
			NOA	Controls
GSE45885	GEO	GPL6244	27	4
GSE45887	GEO	GPL6244	16	4
GSE145467	GEO	GPL4133	10	10
GSE108886	GEO	GPL10558	8	1

GEO, Gene Expression Omnibus; GSE, Gene Expression Omnibus Series; GPL, GEO Platform; NOA, non-obstructive azoospermia.

were applied for screening key genes. The randomForest, e1071, caret packages were employed for RF-RFE and SVM-RFE algorithm construction. Finally, the Venn package was utilized to plot the genes identified by the two algorithms on a Venn diagram, and the intersections were viewed as key genes.

### ***Gene ontology (GO) and Kyoto Encyclopedia of Genes Genomes (KEGG) functional enrichment analysis***

45 genes were copied to the DAVID database (<https://david.ncicrf.gov/>) for GO and KEGG enrichment analyses. A P value <0.05 was set as the filtering threshold, and statistically significant biological process (BP), cellular component (CC), molecular function (MF), and signaling pathways were screened and visualized using the ggplot2 package.

### ***Construction and validation of a nomogram for NOA***

The rms package was adopted for plotting the nomogram, ggplot2, and ggpvr packages for graphing and statistics, the reshape package was used to organize the data for box plots of gene expression, and the ggpvr package was used to compare the mean values of key genes between the two groups. The ComplexHeatmap package was used to draw the heatmap to show the expression differences in three key DEGs between the two groups, and their predictive accuracy for NOA was evaluated.

### ***Validation of candidate genes***

The integrated dataset and external validation set (GSE108886) were used to determine the potential predictive value of candidate genes between NOA and

normal controls. The diagnostic effect was determined based on the AUC of the receiver operating characteristic (ROC) curve. ROC curves of candidate genes were validated using the pROC and ggplot2 program packages.

### ***Immune cell filtration analysis***

Immune infiltration analysis was performed using the CIBERSORT algorithm to assess the infiltration of 22 immune cells in the NOA and control groups (19).

### ***Statistical analysis***

Statistical analyses were done in R (version 4.4.0). Pairwise differences were estimated via the Wilcoxon test. Correlations between genes were judged via Pearson's rank correlation. \*P<0.05 implied statistical significance.

## **Results**

### ***Identification of DEGs and anoikis-related DEGs***

To identify anoikis-related DEGs, we obtained 1,364 DEGs closely related to NOA from the merged test set of 53 NOA samples and 18 normal samples, and up-regulated and downregulated genes were filtered out (*Figure 2A*). There were 919 anoikis-related genes found from the GeneCards database, and 45 anoikis-related DEGs obtained by taking the intersection with 1,364 DEGs from the dataset (*Figure 2B*).

### ***GO and KEGG functional enrichment analyses***

GO analysis elicited that DEGs were highly enriched in BP, like phosphorylation, negative regulation of apoptotic process and cell division; highly enriched in CC, like nucleus, cytosol, and nucleoplasm; highly enriched in MF, like protein binding, ATP binding, and zinc ion binding.

KEGG analysis elicited that DEGs were highly enriched in progesterone-mediated oocyte maturation, mTOR signaling pathway, and FoxO signaling pathway (*Figure 3*).

### ***Potential genes screened by RF-RFE and SVM-RF***

Error rates were plotted against the training set using the randomForest package, yielding the highest diagnostic accuracy at the 66th combination (*Figure 4A*). RF-RFE uncovered nine key genes (*Figure 4B*), which were ranked

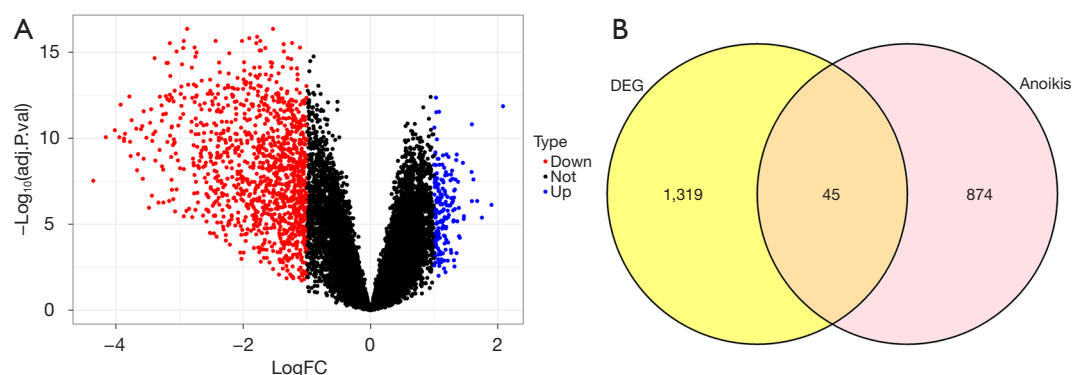


**Figure 2** DEGs in NOA and normal samples. (A) Volcano diagram of DEGs. Red dots signify the significantly downregulated genes, and blue dots signify up-regulated genes. (B) Venn diagram of the 45 anoikis-related DEGs. DEGs, differentially expressed genes; FC, fold change; NOA, non-obstructive azoospermia.

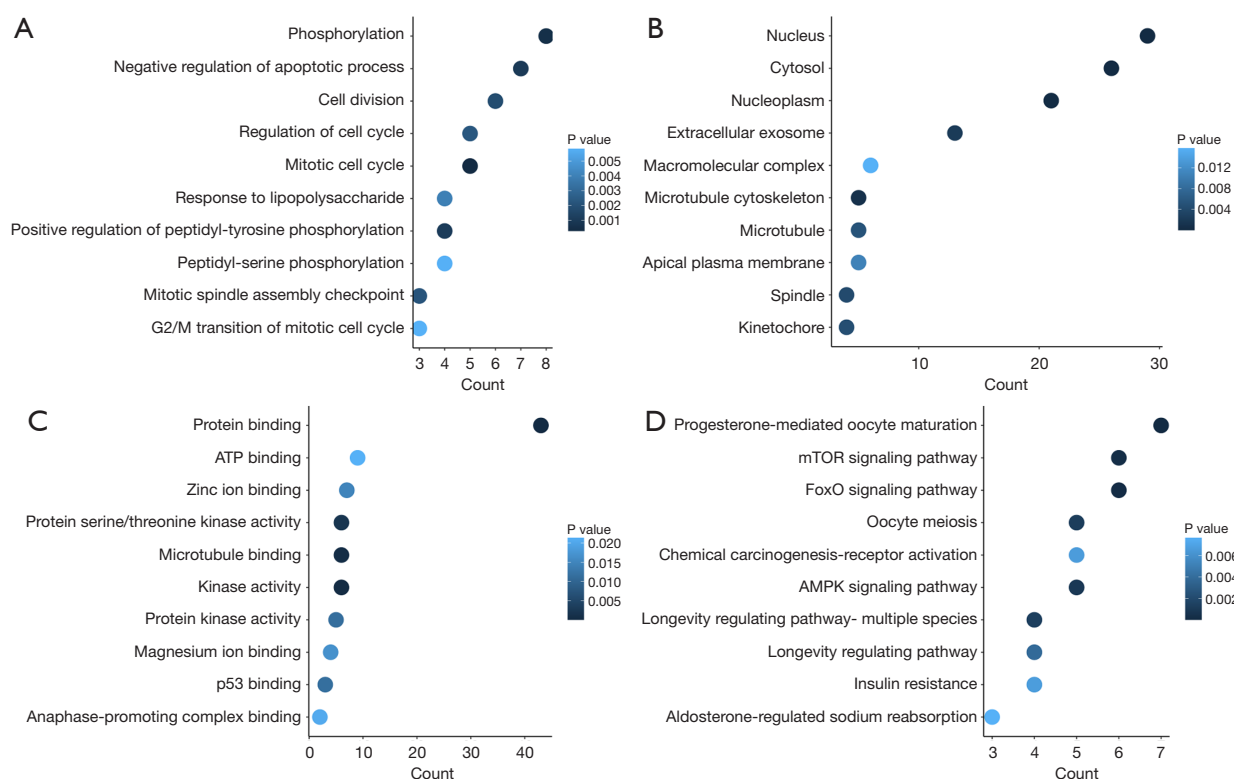


**Figure 3** GO and KEGG functional enrichment analyses. (A) BP that DEGs enriched in. (B) CC that DEGs enriched in. (C) MF that DEGs enriched in. (D) KEGG enrichment results. BP, biological process; CC, cellular component; DEGs, differentially expressed genes; GO, gene ontology; KEGG, Kyoto Encyclopedia of Genes and Genomes; MF, molecular function.

in order of importance, with the top three important genes being *LATS2/ATP6V1F/GLO1* (Figure 4C). 12 genes were filtered out after five cross-validations using *e1071* and *caret* packages (Figure 4D). The 9 genes obtained

by RF and 12 genes obtained by support vector machine (SVM) were taken to intersect and show in a Venn diagram, and 3 candidate genes were screened, *GLO1/BAP1/PLK1* (Figure 4E).

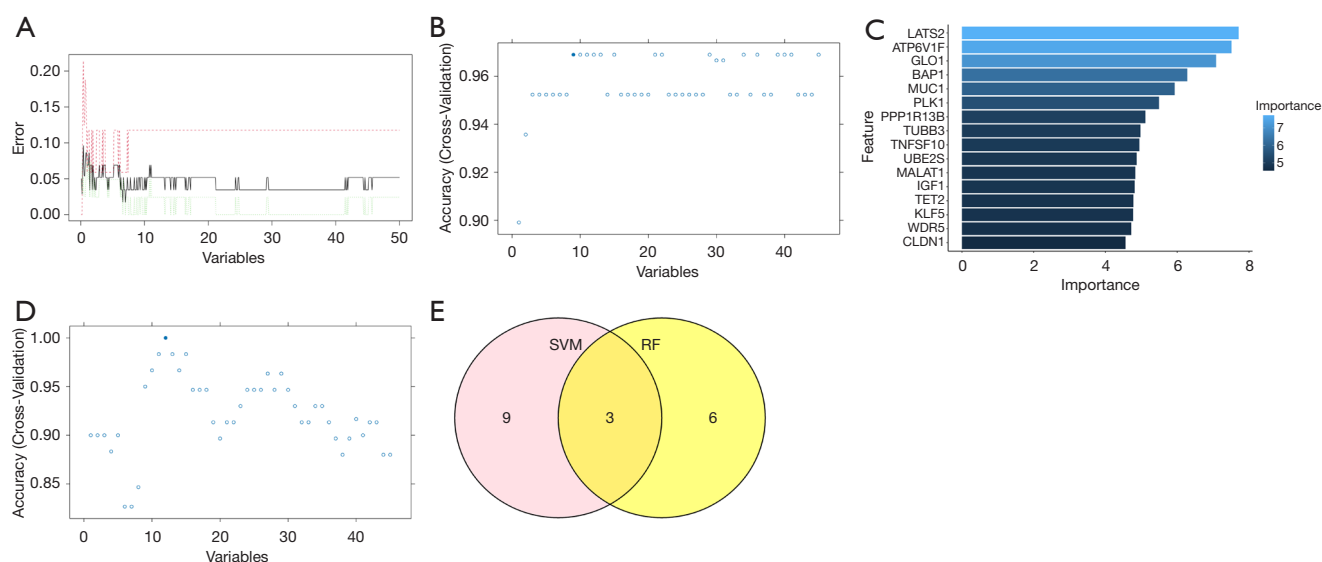


**Figure 4** Three candidate genes were screened using RF and SVM. (A) Error rates were plotted using the randomForest package, and the highest diagnostic accuracy was found at the 66th combination. (B) RF-RFE uncovered nine key genes. (C) The screened key genes were sorted by importance. (D) Twelve key genes were found using SVM. (E) Candidate genes obtained from RF and SVM were intersected to obtain 3 candidate genes. RF, random forest; RF-RFE, random forest-recursive feature elimination; SVM, support vector machine.

### Construction of the nomogram, Boxplot, and complex heatmap

A diagnostic model was developed based on the expression levels of potential biomarkers from the NOA training set (Figure 5A). A nomogram based on the 3 key genes was constructed using the rms package. The calibration curve evinced that the prediction accuracy of the nomogram of 3 key genes was high. The complex heatmap manifested that PLK1 and BAP1 were lowly expressed in the NOA group, and GLO1 was highly expressed (Figure 5B). Boxplots manifested that PLK1 and BAP1 were lowly expressed in the NOA group and GLO1 was highly expressed (Figure 5C).

### Immune cell infiltration analysis

High immune cell infiltration was present in NOA patients, and 16 types of immune cells were significantly different in infiltration between NOA patients and normal controls ( $P < 0.05$ ). Compared to the normal control group, T cells regulatory (Tregs), macrophages M0, macrophages M1, and macrophages M2 were up-regulated in NOA patients, while the other 12 types including T cells CD4 naive and T cells CD4 memory activated were downregulated (Figure 6).

### ROC curves of 3 anoikis-related genes in the iNOA and normal testis tissues

ROC curves disclosed that the AUC of BAP1 was 0.98 (Figure 7A), GLO1 was 0.981 (Figure 7B), and PLK1 was 0.981 (Figure 7C). In the external validation dataset GSE108886, the AUC of BAP1 was 0.875 (Figure 7D), GLO1 was 0.75 (Figure 7E), and PLK1 was 1 (Figure 7F). The three key genes screened by ML algorithms had AUCs greater than 0.7 in both the internal merged dataset and the external validation dataset, indicating high diagnostic efficacy for distinguishing between NOA patients and normal controls.

## Discussion

### Key findings

Male infertility impacts 50% of infertile couples globally, with the most severe form, NOA, affecting 10–15% of infertile males (2). In this paper, a comprehensive bioinformatics approach was leveraged to uncover anoikis-related genes that may serve as potential diagnostic biomarkers for NOA. There were 1,364 DEGs, from which 45 anoikis-related DEGs were filtered through an intersection with anoikis-related genes from the GeneCards



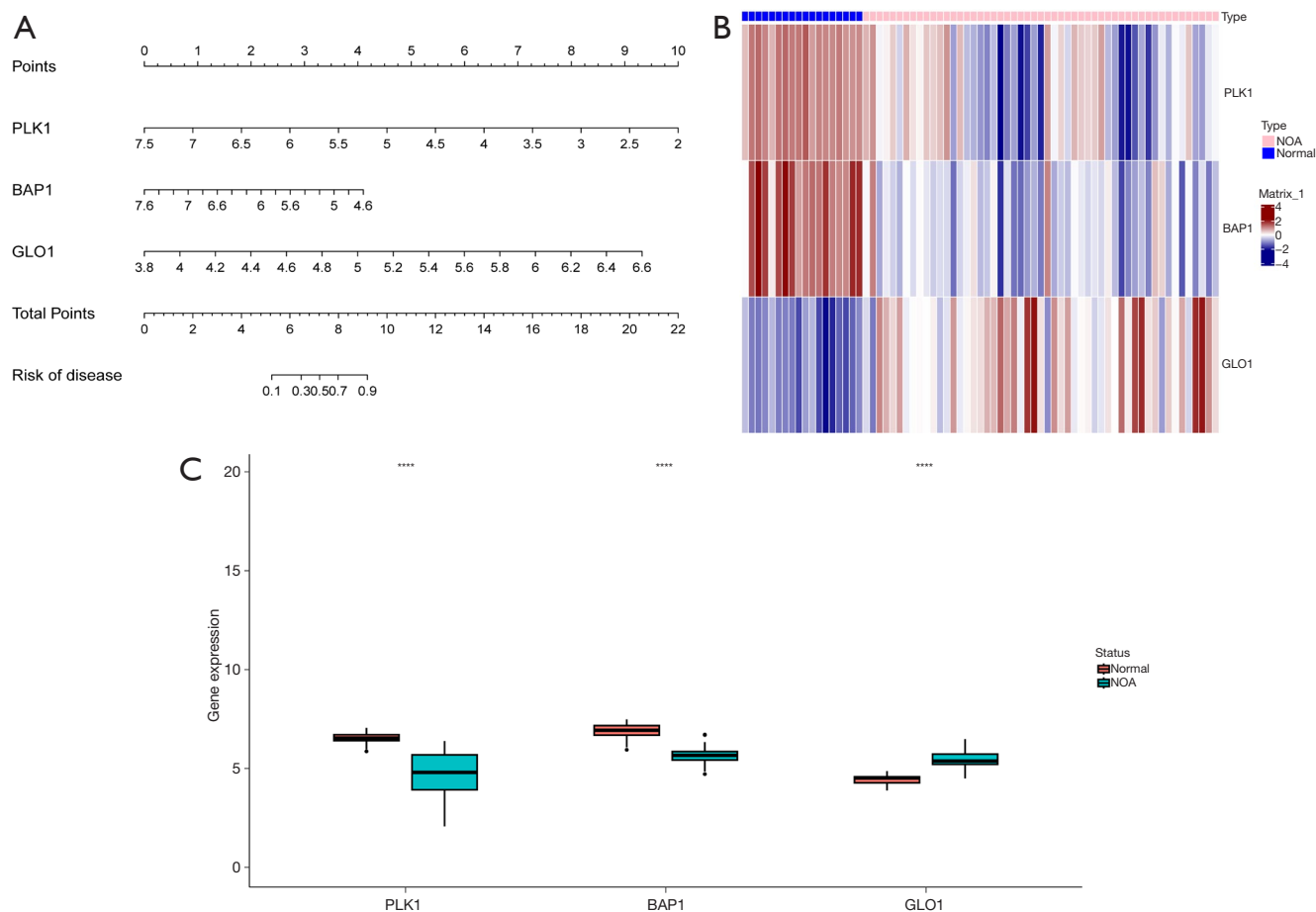


**Figure 5** Construction of the nomogram, Boxplot, and complex heatmap of three key genes. (A) The visible nomogram for diagnosing NOA. (B) Complex heatmaps of the expression of 3 genes in the NOA and normal groups; (C) Boxplots of the expression of 3 candidate genes in the NOA and normal groups. \*\*\*\*,  $P < 0.0001$ . NOA, non-obstructive azoospermia.

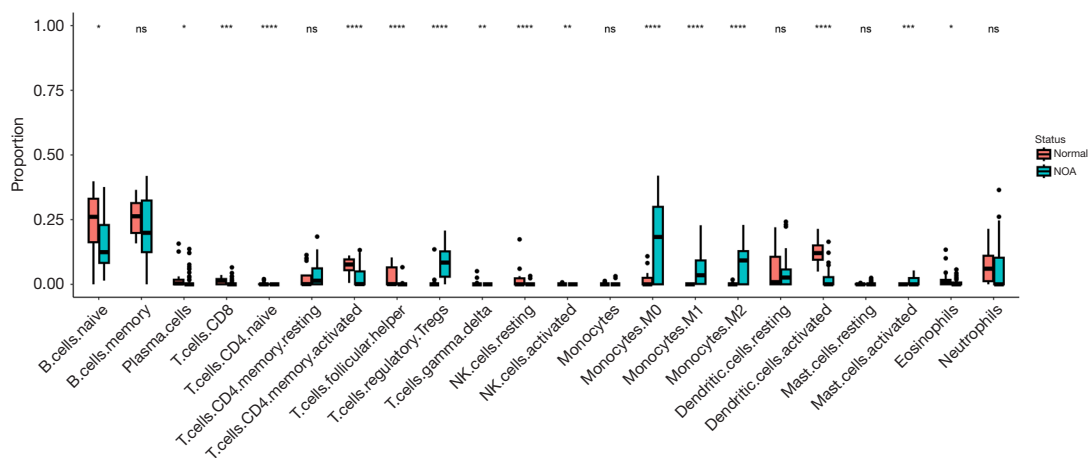


**Figure 6** Immune infiltration analysis. Sixteen immune cells showed significant differences in infiltration between NOA patients and normal controls. \*,  $P < 0.05$ ; \*\*,  $P < 0.01$ ; \*\*\*,  $P < 0.001$ ; \*\*\*\*,  $P < 0.0001$ ; ns, not significant. NOA, non-obstructive azoospermia.

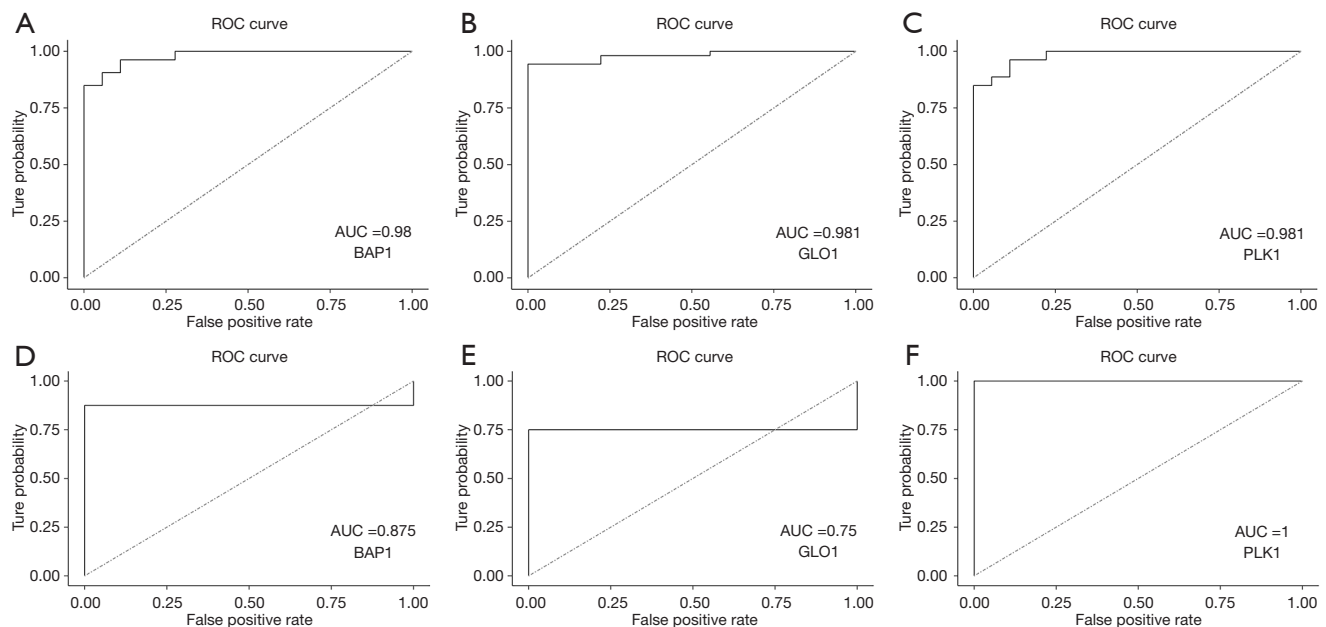


**Figure 7** Diagnostic efficacy and AUC values of 3 key genes in the training set and external validation dataset. The ROC curves of the diagnostic model for 3 key genes in the training set (A-C). The ROC curves of the diagnostic model for 3 key genes in the validation set (D-F). AUC, area under the curve; ROC, receiver operating characteristic.

database. Additionally, ML techniques were adopted to refine our gene selection, ultimately identifying three key candidates: *GLO1*, *BAP1*, and *PLK1*. A nomogram based on these genes demonstrated high predictive accuracy, which was further corroborated by immune cell infiltration analysis and ROC curve evaluations. These findings underline the potential of anoikis-related genes as valuable diagnostic tools in the clinical assessment of NOA, paving the way for future research of targeted therapeutic strategies.

### Strengths and limitations

The methodologies employed in this study exhibited notable strengths in identifying anoikis-related genes associated with NOA. The integration of differential expression analysis with advanced ML techniques facilitated the robust selection of key genes, specifically *GLO1*, *BAP1*, and *PLK1*. Comprehensive bioinformatics tools yielded valuable insights into the BPs and pathways related to NOA. Moreover, a nomogram model based on these critical genes, alongside the validation of their diagnostic efficacy through ROC analysis, highlighted the reliability and predictive power of the identified biomarkers. Collectively, these methodologies enhance our understanding of the molecular mechanisms of NOA and lay the foundation for potential

clinical applications in diagnosis and therapeutic strategies. However, there are certain limitations. Firstly, the absence of experimental validation restricts the confirmatory power of the identified genes and pathways associated with NOA. The reliance on bioinformatics tools, while advantageous for large-scale data analysis, may lead to biases inherent in computational predictions. Furthermore, the relatively small sample size limits the generalizability of our results, potentially overlooking the heterogeneity present in the NOA population. Additionally, variations between datasets could introduce batch effects, complicating the interpretation of results. Future studies should incorporate wet-lab experiments to establish Sertoli-germ cell co-culture models using the three hub genes *GLO1*, *BAP1*, and *PLK1*. Moreover, longitudinal studies that correlate gene expression with testicular sperm extraction (TESE) outcomes, and collaboration with urology centers to obtain larger cohorts of therapeutic biopsy specimens, may enhance the robustness of the findings and validate the identified biomarkers in clinical settings.

### Comparison with similar research

*GLO1*, *BAP1*, and *PLK1* were filtered as key genes associated with NOA, which may offer valuable views into



the molecular mechanisms of NOA. GLO1 is an essential enzyme with pivotal roles in detoxifying methylglyoxal, a byproduct of glycolysis known to induce dicarbonyl stress and apoptosis. GLO1 activity may contribute to renal lipotoxicity linked to diabetes mellitus by activating the NRF2/PI3K/AKT axis (20). Notably, GLO1 overexpression can activate the cell cycle pathway and is positively correlated with numerous key genes related to the cell cycle. Additionally, GLO1 upregulation in hepatocellular carcinoma tissues is associated with dismal outcomes (21). GLO1 knockdown increases advanced glycation end products and activates DNA damage biomarkers, resulting in tumor cell cycle arrest and growth inhibition (22). Conversely, GLO1 overexpression enhances angiogenesis. *In vitro* studies demonstrate that pharmacological inhibition and genetic knockdown of GLO1 in human umbilical vein endothelial cells inhibit proliferation and promote apoptosis (23). Elevated GLO1 levels are correlated with increased cell survival and proliferation, suggesting its potential role in enhancing cellular resilience in the context of NOA. Up-regulated GLO1 observed in our study may reflect a compensatory response to cellular stressors, underscoring its significance as a biomarker for NOA diagnosis and a promising therapeutic target.

BAP1 is a deubiquitinating enzyme with pivotal roles in regulating cell cycle progression and apoptosis. As a recognized tumor suppressor gene, *BAP1* is essential for maintaining cellular integrity (24). Its down-regulation in NOA samples suggests that these critical processes are disrupted, possibly leading to impaired spermatogenesis. Previous studies have stated that BAP1 is involved in the DNA damage response and can influence cellular fate under stress conditions (25-28). Low BAP1 expression in NOA patients may contribute to DNA damage and aggravate the condition. Thus, BAP1 is not only a potential diagnostic marker but also a candidate for targeted therapies aimed at restoring normal cellular functions in NOA.

PLK1 is known to promote cell division and regulate the cell cycle (29), and is extensively studied for its role in mitosis. Research indicates that PLK1 enhances NLRP3 inflammasome activation during the cell interphase (30). Additionally, PLK1 is essential for accurate centromere inheritance and precise chromosome segregation (31,32). DNA polymerase theta is activated by PLK1 during mitosis, highlighting the importance of mitotic double-strand break repair in maintaining genome integrity (33). Notably, the significant downregulation of PLK1 in NOA samples raises concerns regarding its involvement

in spermatogenic failure. Studies have shown that PLK1 is vital for the proper progression of meiosis, and its dysregulation can result in defects in gametogenesis (34-36). Our analysis uncovers *PLK1* as a key gene and emphasizes its potential as both a diagnostic marker and a therapeutic target, suggesting that PLK1 restoration may help mitigate the effects of NOA.

The three key genes identified—*GLO1*, *BAP1*, and *PLK1*—exhibited AUC values exceeding 0.7 in both internal and external validation datasets. This suggests that they may be reliable biomarkers for distinguishing NOA from normal testicular tissues. These findings deepen our comprehension of the molecular mechanisms of NOA and lay the foundation for future research on developing targeted diagnostic and therapeutic strategies.

The progesterone-mediated oocyte maturation pathway is essential for the final stages of oocyte development, which influences ovulation and fertility (37). Dysregulation of this pathway may compromise oocyte quality and maturation processes, leading to reproductive disorders, including NOA (38). Understanding the involvement of this pathway in NOA could provide views for potential therapeutic targets aimed at enhancing fertility.

The mTOR signaling pathway is a central regulator of cell growth, proliferation, and survival, which integrates various environmental signals to modulate cellular functions (39,40). Aberrant activation of this pathway is associated with numerous reproductive disorders, including impaired spermatogenesis (41). The enrichment of DEGs in this pathway in NOA suggests that disruptions in cellular growth and survival may contribute to the pathophysiology of NOA.

The FoxO signaling pathway is recognized for its critical role in regulating apoptosis, oxidative stress response, and cell cycle (42). Its involvement in NOA underscores the significance of cellular stress responses in maintaining spermatogenic health (43). The enrichment of DEGs in this pathway may reflect a diminished capacity to manage cellular stress, thereby contributing to NOA. Functional enrichment analyses further illuminated the BP and MF associated with these DEGs. Notably, the enrichment in phosphorylation and the negative regulation of apoptotic processes suggest that the signaling pathways governing cell survival and death are significantly altered in NOA (44,45). Moreover, the enrichment in the mTOR signaling pathway, which is pivotal in cell growth and metabolism, indicates that metabolic dysregulation may influence NOA pathogenesis (46). Additionally, the FoxO signaling pathway,

implicated in stress resistance and apoptosis, highlights that targeting these pathways may restore normal cellular functions. Understanding these pathways can enhance our comprehension of the molecular mechanisms of NOA and develop targeted therapeutic strategies to restore normal reproductive functions. Further studies are warranted to explore the functional implications of these pathways in NOA and their potential as biomarkers for diagnosis and treatment.

The analysis of immune cell infiltration elicited significant differences in various immune cell types between NOA patients and normal controls. Notably, Tregs were markedly up-regulated in the NOA cohort. Tregs are known for their roles in maintaining immune tolerance and preventing autoimmunity, primarily by secreting anti-inflammatory cytokines and suppressing effector T cell functions. Increased Tregs in NOA patients may suggest an adaptive immune response aimed at modulating inflammation or tissue damage, potentially contributing to NOA (47). This finding aligns with previous studies that have indicated a correlation between Treg levels and various reproductive disorders (48), highlighting the need for further investigations into their roles in NOA. Our results prove that functional changes in several immune cells in the immune microenvironment may be critical for spermatogenesis (49). Additionally, the analysis indicated a significant up-regulation of macrophages, specifically M0, M1, and M2 subtypes, in the NOA group. Macrophages are versatile immune cells that adopt different functional states depending on the microenvironment (50). M1 macrophages are typically linked to pro-inflammatory responses, while M2 macrophages are linked to tissue repair and anti-inflammatory processes (51,52). The observed increases in both M1 and M2 macrophages suggest a complex immune response in NOA, where inflammation and tissue remodeling may coexist. This duality could have implications for therapeutic strategies aimed at modulating macrophage activity to restore normal testicular functions.

In contrast, several immune cell types, including CD4 naive T cells and CD4 memory activated T cells, were found to be down-regulated in the NOA group. This reduction may reflect a compromised adaptive immune response and may prevent effective immune surveillance against pathological changes in the testicular microenvironment (53). Moreover, the observed immune cell infiltration patterns in NOA patients, particularly the up-regulation of Tregs and various macrophage subtypes, suggest a complex interplay between immune response

and anoikis. This correlation may broaden the role of the inflammatory microenvironment in NOA.

### *Explanations of findings*

The identified key signaling pathways associated with DEGs in NOA are pivotal for understanding the underlying mechanisms of NOA. KEGG enrichment analysis revealed three significant pathways: progesterone-mediated oocyte maturation, mTOR signaling pathway, and FoxO signaling pathway, all showing crucial roles in reproductive biology and cellular regulation.

### *Implications and actions needed*

Further investigations are required into the therapeutic implications of these pathways. Collectively, our findings enhance the understanding of the molecular landscape of NOA and pave the way for potential diagnostic and therapeutic strategies by targeting anoikis-related pathways. The influence of anoikis-related genes in the pathogenesis of NOA should be investigated in conjunction with *in vitro* sperm cell culture in future studies. In the next study, we will utilize qPCR and Western blot analyses in biopsy-confirmed NOA cohorts to establish a clinical correlation between biomarker expression and the success rates of microdissection TESE, thereby laying the groundwork for future research to elucidate their mechanistic roles in male infertility.

### **Conclusions**

In conclusion, this study identifies three pivotal genes—*GLO1*, *BAP1*, and *PLK1*—that demonstrate robust diagnostic potential and underscore the BPs and associated pathways relevant to the molecular mechanisms of NOA. These genes may be biomarkers for early diagnosis and treatment. The insights gained from our comprehensive bioinformatics analysis enrich the understanding of the disease's pathogenesis and offer references for future research. Ultimately, incorporating these findings into clinical practice could significantly enhance the diagnostic and therapeutic landscape for NOA patients, thereby improving male reproductive health.

### **Acknowledgments**

None.

## Footnote

**Reporting Checklist:** The authors have completed the STARD reporting checklist. Available at <https://tau.amegroups.com/article/view/10.21037/tau-2024-745/rc>

**Peer Review File:** Available at <https://tau.amegroups.com/article/view/10.21037/tau-2024-745/prf>

**Funding:** This work was supported by Weifang Fundamental Research Projects (grant No. WFWSJK-2023-052).

**Conflicts of Interest:** All authors have completed the ICMJE uniform disclosure form (available at <https://tau.amegroups.com/article/view/10.21037/tau-2024-745/coif>). The authors have no conflicts of interest to declare.

**Ethical Statement:** The authors are accountable for all aspects of the work in ensuring that questions related to the accuracy or integrity of any part of the work are appropriately investigated and resolved. The study was conducted in accordance with the Declaration of Helsinki and its subsequent amendments.

**Open Access Statement:** This is an Open Access article distributed in accordance with the Creative Commons Attribution-NonCommercial-NoDerivs 4.0 International License (CC BY-NC-ND 4.0), which permits the non-commercial replication and distribution of the article with the strict proviso that no changes or edits are made and the original work is properly cited (including links to both the formal publication through the relevant DOI and the license). See: <https://creativecommons.org/licenses/by-nc-nd/4.0/>.

## References

1. Cox CM, Thoma ME, Tchangalova N, et al. Infertility prevalence and the methods of estimation from 1990 to 2021: a systematic review and meta-analysis. *Hum Reprod Open* 2022;2022:hoac051.
2. Piechka A, Sparanese S, Witherspoon L, et al. Molecular mechanisms of cellular dysfunction in testes from men with non-obstructive azoospermia. *Nat Rev Urol* 2024;21:67-90.
3. Schlegel PN, Sigman M, Collura B, et al. Diagnosis and Treatment of Infertility in Men: AUA/ASRM Guideline PART II. *J Urol* 2021;205:44-51.
4. Schlegel PN, Sigman M, Collura B, et al. Diagnosis and treatment of infertility in men: AUA/ASRM guideline part I. *Fertil Steril* 2021;115:54-61.
5. Mei J, Jiang XY, Tian HX, et al. Anoikis in cell fate, physiopathology, and therapeutic interventions. *MedComm* (2020) 2024;5:e718.
6. Frisch SM, Francis H. Disruption of epithelial cell-matrix interactions induces apoptosis. *J Cell Biol* 1994;124:619-26.
7. Wang LN, Zhang ZT, Wang L, et al. TGF- $\beta$ 1/SH2B3 axis regulates anoikis resistance and EMT of lung cancer cells by modulating JAK2/STAT3 and SHP2/Grb2 signaling pathways. *Cell Death Dis* 2022;13:472.
8. Li T, Yu Y, Song Y, et al. Activation of BDNF/TrkB pathway promotes prostate cancer progression via induction of epithelial-mesenchymal transition and anoikis resistance. *FASEB J* 2020;34:9087-101.
9. Tan M, Asad M, Heong V, et al. The FZD7-TWIST1 axis is responsible for anoikis resistance and tumorigenesis in ovarian carcinoma. *Mol Oncol* 2019;13:757-80.
10. Doxtater K, Tripathi MK, Sekhri R, et al. MUC13 drives cancer aggressiveness and metastasis through the YAP1-dependent pathway. *Life Sci Alliance* 2023;6:e202301975.
11. Moreira S, Martins AD, Alves MG, et al. Aminocarb Exposure Induces Cytotoxicity and Endoplasmic Reticulum Stress-Mediated Apoptosis in Mouse Sustentacular Sertoli Cells: Implications for Male Infertility and Environmental Health. *Biology (Basel)* 2024;13:721.
12. Clough E, Barrett T, Wilhite SE, et al. NCBI GEO: archive for gene expression and epigenomics data sets: 23-year update. *Nucleic Acids Res* 2024;52:D138-44.
13. Davis S, Meltzer PS. GEOquery: a bridge between the Gene Expression Omnibus (GEO) and BioConductor. *Bioinformatics* 2007;23:1846-7.
14. Chen C, Grennan K, Badner J, et al. Removing batch effects in analysis of expression microarray data: an evaluation of six batch adjustment methods. *PLoS One* 2011;6:e17238.
15. Leek JT, Johnson WE, Parker HS, et al. The sva package for removing batch effects and other unwanted variation in high-throughput experiments. *Bioinformatics* 2012;28:882-3.
16. Smyth GK. Linear models and empirical bayes methods for assessing differential expression in microarray experiments. *Stat Appl Genet Mol Biol* 2004;3:Article3.
17. Lin X, Li C, Zhang Y, et al. Selecting Feature Subsets Based on SVM-RFE and the Overlapping Ratio with Applications in Bioinformatics. *Molecules* 2017;23:52.

18. Alakwaa FM, Chaudhary K, Garmire LX. Deep Learning Accurately Predicts Estrogen Receptor Status in Breast Cancer Metabolomics Data. *J Proteome Res* 2018;17:337-47.
19. Chen B, Khodadoust MS, Liu CL, et al. Profiling Tumor Infiltrating Immune Cells with CIBERSORT. *Methods Mol Biol* 2018;1711:243-59.
20. Peng CC, Chen ECY, Chen CR, et al. Molecular mechanism of ectopic lipid accumulation induced by methylglyoxal via activation of the NRF2/PI3K/AKT pathway implicates renal lipotoxicity caused by diabetes mellitus. *PLoS One* 2024;19:e0306575.
21. Zhang Y, Tang X, Liu L, et al. GLO1 regulates hepatocellular carcinoma proliferation and migration through the cell cycle pathway. *BMC Cancer* 2024;24:1297.
22. Hu L, Xie K, Zheng C, et al. Exosomal MALAT1 promotes the proliferation of esophageal squamous cell carcinoma through glyoxalase 1-dependent methylglyoxal removal. *Noncoding RNA Res* 2024;9:330-40.
23. Wan YX, Qi XW, Lian YY, et al. Electroacupuncture facilitates vascular normalization by inhibiting Glyoxalase1 in endothelial cells to attenuate glycolysis and angiogenesis in triple-negative breast cancer. *Cancer Lett* 2024;598:217094.
24. Lalloo F, Kulkarni A, Chau C, et al. Clinical practice guidelines for the diagnosis and surveillance of BAP1 tumour predisposition syndrome. *Eur J Hum Genet* 2023;31:1261-9.
25. Guazzelli A, Meysami P, Bakker E, et al. BAP1 Status Determines the Sensitivity of Malignant Mesothelioma Cells to Gemcitabine Treatment. *Int J Mol Sci* 2019;20:429.
26. Fukuda T, Tsuruga T, Kuroda T, et al. Functional Link between BRCA1 and BAP1 through Histone H2A, Heterochromatin and DNA Damage Response. *Curr Cancer Drug Targets* 2016;16:101-9.
27. Carbone M, Harbour JW, Brugarolas J, et al. Biological Mechanisms and Clinical Significance of BAP1 Mutations in Human Cancer. *Cancer Discov* 2020;10:1103-20.
28. Lee SA, Lee D, Kang M, et al. BAP1 promotes the repair of UV-induced DNA damage via PARP1-mediated recruitment to damage sites and control of activity and stability. *Cell Death Differ* 2022;29:2381-98.
29. Iliaki S, Beyaert R, Afonina IS. Polo-like kinase 1 (PLK1) signaling in cancer and beyond. *Biochem Pharmacol* 2021;193:114747.
30. Baldrighi M, Doreth C, Li Y, et al. PLK1 inhibition dampens NLRP3 inflammasome-elicited response in inflammatory disease models. *J Clin Invest* 2023;133:e162129.
31. Conti D, Verza AE, Pesenti ME, et al. Role of protein kinase PLK1 in the epigenetic maintenance of centromeres. *Science* 2024;385:1091-7.
32. Parashara P, Medina-Pritchard B, Abad MA, et al. PLK1-mediated phosphorylation cascade activates Mis18 complex to ensure centromere inheritance. *Science* 2024;385:1098-104.
33. Gelot C, Kovacs MT, Miron S, et al. Polθ is phosphorylated by PLK1 to repair double-strand breaks in mitosis. *Nature* 2023;621:415-22.
34. Wellard SR, Skinner MW, Zhao X, et al. PLK1 depletion alters homologous recombination and synaptonemal complex disassembly events during mammalian spermatogenesis. *Mol Biol Cell* 2022;33:ar37.
35. Menon DU, Kirsanov O, Geyer CB, et al. Mammalian SWI/SNF chromatin remodeler is essential for reductional meiosis in males. *Nat Commun* 2021;12:6581.
36. Feitosa WB, Hwang K, Morris PL. Temporal and SUMO-specific SUMOylation contribute to the dynamics of Polo-like kinase 1 (PLK1) and spindle integrity during mouse oocyte meiosis. *Dev Biol* 2018;434:278-91.
37. Clark HM, Stokes AE, Edwards JL, et al. Impact of preovulatory follicle maturity on oocyte metabolism and embryo development. *PNAS Nexus* 2024;3:pgae181.
38. Li H, Liu J, Nong W, et al. Aluminum exposure impairs oocyte quality via subcellular structure disruption and DNA damage-related apoptosis in mice. *J Environ Sci (China)* 2024;139:308-19.
39. Kim J, Guan KL. mTOR as a central hub of nutrient signalling and cell growth. *Nat Cell Biol* 2019;21:63-71.
40. Zhao T, Fan J, Abu-Zaid A, et al. Nuclear mTOR Signaling Orchestrates Transcriptional Programs Underlying Cellular Growth and Metabolism. *Cells* 2024;13:781.
41. Wang LM, Jia K, Li ZF, et al. TiO<sub>2</sub> nanoparticles affect spermatogenesis and adhesion junctions via the ROS-mediated mTOR signalling pathway in Eriocheir sinensis testes. *Environ Pollut* 2023;331:121952.
42. Rodriguez-Colman MJ, Dansen TB, Burgering BMT. FOXO transcription factors as mediators of stress adaptation. *Nat Rev Mol Cell Biol* 2024;25:46-64.
43. Ge P, Zhang J, Zhou L, et al. CircRNA expression profile and functional analysis in testicular tissue of patients with non-obstructive azoospermia. *Reprod Biol Endocrinol* 2019;17:100.

44. Li N, Zhou Q, Yi Z, et al. Ubiquitin protein E3 ligase ASB9 suppresses proliferation and promotes apoptosis in human spermatogonial stem cell line by inducing HIF1AN degradation. *Biol Res* 2023;56:4.
45. Liu X, Zang C, Wu Y, et al. Homeodomain-interacting protein kinase HIPK4 regulates phosphorylation of manchette protein RIMBP3 during spermiogenesis. *J Biol Chem* 2022;298:102327.
46. Fang X, Lu X, Ma Y, et al. Possible involvement of a MEG3-miR-21-SPRY1-NF- $\kappa$ B feedback loop in spermatogenic cells proliferation, autophagy, and apoptosis. *iScience* 2024;27:110904.
47. Luo X, Zheng H, Nai Z, et al. Identification of biomarkers associated with macrophage infiltration in non-obstructive azoospermia using single-cell transcriptomic and microarray data. *Ann Transl Med* 2023;11:55.
48. Zhong Y, Zhao J, Deng H, et al. Integrative bioinformatics analysis to identify novel biomarkers associated with non-obstructive azoospermia. *Front Immunol* 2023;14:1088261.
49. Zhong Y, Chen X, Zhao J, et al. Integrative analyses of potential biomarkers and pathways for non-obstructive azoospermia. *Front Genet* 2022;13:988047.
50. Dong M, Li H, Zhang X, et al. Weighted Correlation Gene Network Analysis Reveals New Potential Mechanisms and Biomarkers in Non-obstructive Azoospermia. *Front Genet* 2021;12:617133.
51. Wu H, Zheng J, Xu S, et al. Mer regulates microglial/macrophage M1/M2 polarization and alleviates neuroinflammation following traumatic brain injury. *J Neuroinflammation* 2021;18:2.
52. Yunna C, Mengru H, Lei W, et al. Macrophage M1/M2 polarization. *Eur J Pharmacol* 2020;877:173090.
53. Hunt PW, Landay AL, Sinclair E, et al. A low T regulatory cell response may contribute to both viral control and generalized immune activation in HIV controllers. *PLoS One* 2011;6:e15924.

**Cite this article as:** Xu X, Xie J, Cheng W. Novel anoikis-related genes for the diagnosis of non-obstructive azoospermia. *Transl Androl Urol* 2025;14(4):940-952. doi: 10.21037/tau-2024-745